ON THE MOVE: LOCALIZATION WITH KINETIC EUCLIDEAN DISTANCE MATRICES

Puoya Tabaghi ⋆ *Ivan Dokmanić* ⋆ *Martin Vetterli*†

⋆ University of Illinois at Urbana-Champaign, USA
† Ecole polytechnique fédérale de Lausanne, Switzerland
⋆{tabaghi2, dokmanic}@illinois.edu, †martin.vetterli@epfl.ch

ABSTRACT

In this paper, we propose kinetic Euclidean distance matrices (KEDMs)—a new algebraic tool for localization of moving points from spatio–temporal distance measurements. KEDMs are inspired by the well-known Euclidean distance matrices (EDM) which model static points. When objects move, trajectory models may enable better localization from fewer samples by trading off samples in space for samples in time. We develop the theory for polynomial trajectory models used in tracking and simultaneous localization and mapping. Concretely, we derive a semidefinite relaxation for KEDMs inspired by similar algorithms for the usual EDMs, and propose a new spectral factorization algorithm adapted to trajectory reconstruction. Numerical experiments show that KEDMs and the new semidefinite relaxation accurately reconstruct trajectories from incomplete, noisy distance observations, scattered over multiple time instants. In particular, they show that temporal oversampling can considerably reduce the required number of measured distances at any given time.

Index Terms— Euclidean distance matrix, semidefinite programming, trajectory localization, polynomial spectral factorization.

1. INTRODUCTION

The famous distance geometry problem (DGP) [1] asks to reconstruct the geometry of a point set from a subset of interpoint distances. The DGP models sensor network localization [2], microphone positioning [3, 4, 5], clock synchronization [6] and molecular geometry reconstruction from nuclear magnetic resonance (NMR) data [7, 8, 9]. Euclidean distance matrices (EDMs) are among the most successful tools used to design DGP algorithms.

The study of distance geometry and EDMs goes back to the works of Menger [10], Schoenberg [11], Blumenthal [12], and Young and Householder [13]. Many theoretical results on EDMs including the rank characterization were derived by Gower [14, 15]. An extensive treatise with many original results and an elegant characterization of the EDM cone was written by Dattorro [16]; a tutorial-style introduction is given in [17]. When objects move, EDMs only characterize a snapshot of interpoint distances. They can be used to recover the point set geometry at each time independently. It seems intuitive that with a good trajectory model, one should be able to leverage the motion and improve localization, as in [21].

In this paper, we introduce kinetic EDMs (KEDMs) and show how to use them to address kinetic distance geometry problems, defined in Section 2. For the class of polynomial trajectories, we show how to systematically estimate the time-varying point locations by measuring subsets of pairwise distances. Moreover, we show that this is possible even when the number of measured distances at any given time is too small to localize in the static case.

Localization of moving objects from distances is useful in a number of applications. Robot swarms, for example, must often localize autonomously [18], especially in remote situations such as extraterrestrial exploration [19], deep-water missions [20]. In some emerging applications sensing is opportunistic and the positions of reference objects are not known [22]. This problem is further related to simultaneous localization and mapping (SLAM) [23, 24].

A large class of approaches to point set localization from interpoint distances rely on semidefinite programming [25, 26]. We take inspiration from these approaches and show that with some work, trajectory localization can also be formulated as a semidefinite program. Concretely, we show that parameters of the chosen trajectory model can be recovered by a semidefinite relaxation and a tailor-made alignment procedure akin to Procrustes analysis. The latter can be interpreted as spectral factorization of semidefinite polynomial matrices with side information corresponding to anchor locations.

We show through extensive computer experiments that through our proposed method we can indeed accurately reconstruct trajectories from noisy and missing distances and reduce the number of measurements *per time instant* by spreading the measurements in time.

2. STATIC AND KINETIC DISTANCE GEOMETRY PROBLEMS

We begin by introducing the classical distance geometry problem (DGP) and then generalize it to points moving along trajectories. We let $\mathcal{E}_N$ denote the set of all index pairs for N points, $\mathcal{E}_N \stackrel{\text{def}}{=} \{(m,n) : 1 \leq m < n \leq N\}$ and define:

Problem 1 (Distance Geometry Problem)**.** *Given an embedding dimension $d > 0$ and a subset of pairwise distances $\mathcal{S} = \{d_{mn} : (m,n) \subseteq E\}$, determine whether there are points $\{\boldsymbol{x}_n\}_{n=1}^N$ in dimension d such that $d_{mn} = \|\boldsymbol{x}_m - \boldsymbol{x}_n\|$ for all $(m,n) \in \mathcal{S}$.*

In practice the measurements are often corrupted by noise, in which case the goal is to minimize some notion of discrepancy between the measured and estimated distances.

The kinetic distance geometry problem (KDGP) asks to estimate entire trajectories, in contrast to DGP where we localize the points only at measurement times. For KDGP to be well-defined, we need to introduce a class of admissible trajectories (a trajectory model) $\mathcal{X}$. In this paper we work with a polynomial $\mathcal{X}$.

Problem 2 (Kinetic Distance Geometry Problem)**.** *Given an embedding dimension $d > 0$, a set of T sampling times $\mathcal{T}_s = \{t_1, \ldots, t_T\}$, and a subset of pairwise distance measurements $\mathcal{S}(t_i) = \{d_{mn}(t_i) : (m,n) \in E_N\}$ at each sampling time, determine whether there is a trajectory set $\boldsymbol{X} : \mathcal{T} \to \mathbb{R}^{d \times N} \in \mathcal{X}$ such*

978-1-5386-4658-8/18/$31.00 ©2019 IEEE

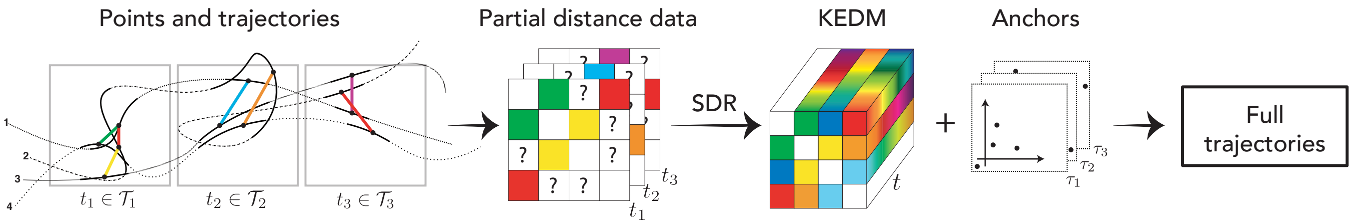

Fig. 1: Illustration of the trajectory estimation pipeline using KEDMs. The data consists of pairwise distance measurements distributed in space and time. The distances are fed into a semidefinite relaxation which outputs a KEDM (Section 4). Finally, anchor point locations at a set of L times are used to estimate the trajectories by an informed spectral factorization algorithm (Section 4.1).

that for all $t_i \in \mathcal{T}_s$ and for all measurements at time t_i, we have $\|\boldsymbol{x}_m(t_i) - \boldsymbol{x}_n(t_i)\| = d_{mn}(t_i)$ for all $(m, n) \in \mathcal{S}(t_i)$.

Figure 1 illustrates the KDGP and the proposed solution for four trajectories; We can interpret KDGP is as sequence of static DGPs with additional information about the sampling times and the trajectory model.

2.1. Solving the Distance Geometry Problem by EDMs

We start by recalling the EDM-based approach to the DGP. Let us ascribe the coordinates of N points in a d-dimensional space to the columns of matrix $\boldsymbol{X} \in \mathbb{R}^{d\times N}$, $\boldsymbol{X} = [\boldsymbol{x}_1, \ \boldsymbol{x}_2, \ \cdots, \ \boldsymbol{x}_N]$. The corresponding Euclidean distance matrix (EDM) $\boldsymbol{D} = (\|\boldsymbol{x}_i - \boldsymbol{x}_j\|^2)_{ij}$ can be written as [17]

$$\boldsymbol{D} = \mathcal{K}(\boldsymbol{G}) \stackrel{\text{def}}{=} \operatorname{diag}(\boldsymbol{G})\boldsymbol{1}^\top - 2\boldsymbol{G} + \boldsymbol{1}\operatorname{diag}(\boldsymbol{G})^\top, \qquad (1)$$

where $\boldsymbol{1}$ denotes the column vector of all ones, $\boldsymbol{G}$ is the Gram matrix $\boldsymbol{G} = \boldsymbol{X}^\top\boldsymbol{X}$, and $\operatorname{diag}(\boldsymbol{G})$ is a column vector of the diagonal entries of $\boldsymbol{G}$. Let $\widetilde{\boldsymbol{D}}$ be a noisy, incomplete EDM with unknown entries replaced by zeros. Then using (1), we can write the following semidefinite program to complete and denoise $\widetilde{\boldsymbol{D}}$:

$$\begin{array}{ll} \underset{\boldsymbol{G}}{\text{minimize}} & \|\widetilde{\boldsymbol{D}} - \boldsymbol{W} \circ \mathcal{K}(\boldsymbol{G})\|_F^2 \\ \text{subject to} & \boldsymbol{G} \succeq \boldsymbol{0} \\ & \boldsymbol{G}\boldsymbol{1} = \boldsymbol{0} \\ & \operatorname{rank}(\boldsymbol{G}) \leq d, \end{array} \qquad (2)$$

where $\boldsymbol{W} \in \{0, 1\}^{N\times N}$ is a binary mask matrix whose non-zero entries correspond to the known distances and $\circ$ denotes the entrywise product. While the objective in (2) is convex (because $\mathcal{K}$ is linear in the Gram matrix), the rank constraint makes the feasible non-convex. Removing the rank constraint leads to a standard semidefinite relaxation which is known to perform well so long as the number of points is not too small [17, 25]. Once the Gram matrix is found, we estimate the point locations $\widehat{\boldsymbol{X}}$ by an eigenvalue decomposition from $\boldsymbol{G} = \boldsymbol{X}^\top\boldsymbol{X}$. Since the EDM only specifies the points up to a rigid transformation, $\widehat{\boldsymbol{X}}$ will be a rotated, reflected and translated version of $\boldsymbol{X}$. The constraint $\boldsymbol{G}\boldsymbol{1} = \boldsymbol{0}$ fixes the centroid $\widehat{\boldsymbol{X}}$ at the origin since it implies $\boldsymbol{X}\boldsymbol{1} = \boldsymbol{0}$. A standard method to recover the absolute locations is to use known anchor points.

2.2. Orthogonal Procrustes Problem

Let $\boldsymbol{X}_a \in \mathbb{R}^{d\times N_a}$, $N_a \geq d+1$, be a submatrix (a selection of columns) of $\boldsymbol{X}$ that is to be aligned with N_a anchor points with known positions listed as columns of $\boldsymbol{Y} \in \mathbb{R}^{d\times N_a}$. The least-squares rigid alignment can be computed in two steps. We first center the columns of $\boldsymbol{Y}$ and $\boldsymbol{X}_a$ by subtracting the corresponding column centroids $\boldsymbol{x}_{a,c}$ and $\boldsymbol{y}_c$ to get $\overline{\boldsymbol{Y}}$ and $\overline{\boldsymbol{X}}_a$, and then search for the rotation and reflection that best maps $\overline{\boldsymbol{X}}_a$ onto $\overline{\boldsymbol{Y}}$. The second step is known as orthogonal Procrustes analysis [27]. Let $\boldsymbol{U}\boldsymbol{\Sigma}\boldsymbol{V}^\top$ be the SVD of $\overline{\boldsymbol{X}}_a\overline{\boldsymbol{Y}}^\top$. The optimal rotation is given as $\boldsymbol{R} \stackrel{\text{def}}{=} \boldsymbol{V}\boldsymbol{U}^\top$ and alignment is applied to the reconstructed point set as

$$\boldsymbol{X}_{\text{aligned}} = \boldsymbol{R}(\boldsymbol{X} - \boldsymbol{x}_{a,c}\boldsymbol{1}^\top) + \boldsymbol{y}_c\boldsymbol{1}^\top.$$

We will use this method to devise an alignment procedure with moving anchors in Section 4.1.

3. KINETIC EDMS AND BASIS GRAMIANS

Let $\boldsymbol{X}(t) = [\boldsymbol{x}_1(t), \ldots, \boldsymbol{x}_N(t)]$ be the trajectory matrix of N moving points in $\mathbb{R}^d$, where $\boldsymbol{x}_n(t)$ is the position of the nth point at time t. We define the corresponding KEDM in a natural way:

Definition 1 (KEDM)**.** *Given a set of trajectories $\boldsymbol{X}(t) \in \mathbb{R}^{d\times N}[t]$, the corresponding KEDM is the time-dependent matrix $\boldsymbol{D}(t) \in \mathbb{R}^{N\times N}[t]$ of time-varying squared distances between the points:*

$$\boldsymbol{D}(t) \stackrel{\text{def}}{=} \mathcal{D}(\boldsymbol{X}(t)),$$

where $\mathcal{D}(\boldsymbol{X}(t)) = \mathcal{K}(\boldsymbol{X}(t)^\top\boldsymbol{X}(t))$

For a set of N points in $\mathbb{R}^d$, we define the set of polynomial trajectories of degree P as

$$\mathcal{X}_{\text{poly}} = \left\{ \sum_{p=0}^{P} t^p \boldsymbol{A}_p \,\middle|\, \boldsymbol{A}_p \in \mathbb{R}^{d\times N}, \ p \in \{0, \ldots, P\} \right\}. \qquad (3)$$

This model is common in tracking and SLAM, e.g., as a constant velocity or constant acceleration assumption [28, 29].

Similar to the static case, our goal is to cast the trajectory retrieval problem as a semidefinite program. A central role is again played by the Gram matrix which now becomes a function of time,

$$\boldsymbol{G}(t) = \boldsymbol{X}(t)^\top\boldsymbol{X}(t) = \sum_{k=0}^{K} \boldsymbol{B}_k t^k, \qquad (4)$$

where $\boldsymbol{B}_k \stackrel{\text{def}}{=} \sum_{p=0}^{k} \boldsymbol{A}_p^\top \boldsymbol{A}_{k-p}$ and $K = 2P$.

It is useful to reduce time-varying localization to a problem that only involves constant Gram matrices. To this end, the following proposition lets us express the time-dependent Gramian of a polynomial trajectory set in terms of K constant *basis* Gramians $\boldsymbol{G}_k$:

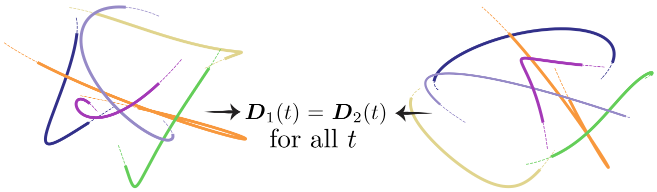

Fig. 2: Two set of trajectories which are not rigid transforms of each other, but generate the same KEDM. Corresponding points have the same color.

Proposition 1. *Consider the polynomial trajectory in* (3). *Let* $\boldsymbol{G}_k \overset{def}{=} \boldsymbol{G}(\tau_k),\ k \in \{0, 1, \ldots, K\},\ K = 2P$, *with all* τ_k *distinct. Then*

$$\boldsymbol{G}(t) = \sum_{k=0}^{K} w_k(t) \boldsymbol{G}_k, \tag{5}$$

with the weights $\boldsymbol{w}(t) = [w_0(t), \cdots, w_K(t)]^\top$ *given as*

$$\boldsymbol{w}(t) = \begin{pmatrix} 1 & 1 & \cdots & 1 \\ \vdots & \vdots & \ddots & \vdots \\ \tau_0^K & \tau_1^K & \cdots & \tau_K^K \end{pmatrix}^{-1} \begin{pmatrix} 1 \\ t \\ \vdots \\ t^K \end{pmatrix}.$$

Proof. The Gramian can be written as a linear combination of a set of monomial terms (cf. (4)), which gives

$$\boldsymbol{G}_k = \boldsymbol{B}_0 + \tau_k \boldsymbol{B}_1 + \cdots + \tau_k^K \boldsymbol{B}_K,\ k \in \{0, \cdots, K\} \tag{6}$$

Each matrix equation in (6) consists of $N \times N$ scalar equations for entries of $\boldsymbol{G}_k$. Focusing on a particular entry (i, j) gives a usual linear system $\boldsymbol{g} = \boldsymbol{M}\boldsymbol{b}$ with column vector $\boldsymbol{g} = [g_0, \cdots, g_K]^\top$ where g_k is (i, j)-th element of $\boldsymbol{G}_k$, the matrix $\boldsymbol{M} \overset{\text{def}}{=} [\tau_k^{k'}]_{0 \le k, k' \le K}$, and $\boldsymbol{b} = [b_0, \cdots, b_K]^\top$ where b_k is (i, j)-th element of $\boldsymbol{B}_k$. We also have from (4) that $[\boldsymbol{G}(t)]_{ij} = (1, t, t^2, \ldots, t^K)\boldsymbol{b} \overset{\text{def}}{=} \boldsymbol{t}^\top \boldsymbol{b}$. Since τ_k are distinct, the square Vandermonde matrix $\boldsymbol{M}$ is invertible. We have $\boldsymbol{b} = \boldsymbol{M}^{-1}\boldsymbol{g}$, which gives $[\boldsymbol{G}(t)]_{ij} = \boldsymbol{t}^\top \boldsymbol{M}^{-1}\boldsymbol{g}$. Denoting $\boldsymbol{w}(t) = (\boldsymbol{M}^\top)^{-1}\boldsymbol{t}$ we have that $[\boldsymbol{G}(t)]_{ij} = \boldsymbol{w}(t)^\top \boldsymbol{g} = \sum_{k=0}^{K} w_k(t)[\boldsymbol{G}_k]_{ij}$ which proves the claim. □

Same as in the static DGP, the KDGP suffers from rigid transformation ambiguity. However, since at every time instant we can apply a different rigid transform, the set of ambiguities that arise in the KDGP is much larger than just the rigid transforms of trajectories. In particular, rather different trajectories (nothing like rotations and translations of each other) can generate the same KEDM, as illustrated Figure 2. We discuss this problem further in Section 4.1, where we propose a method for spectral factorization of kinetic Gramians that resolves the described ambiguities.

4. TRAJECTORY LOCALIZATION BY KINETIC EDMS

The basis Gramian representation (5) allows us to formulate a semidefinite program inspired by (2) for the trajectory recovery problem. Denote the sequence of incomplete, noisy EDMs at times $\{t_i\}_{i=1}^T$ by $\{\widetilde{\boldsymbol{D}}_i\}_{i=1}^T$, and the corresponding measurement masks by $\{\boldsymbol{W}_i\}_{i=1}^T$. In analogy with (2), we propose to solve: [1]

$$\begin{aligned} \underset{(\boldsymbol{G}_k : \boldsymbol{G}_k \succeq 0)_{k=0}^K}{\text{minimize}} \quad & \sum_{i=1}^{T} \alpha_i \left\| \widetilde{\boldsymbol{D}}_i - \boldsymbol{W}_i \circ \mathcal{K}\left(\sum_{k=0}^{K} w_k(t_i) \boldsymbol{G}_k \right) \right\|_F^2 \\ \text{subject to} \quad & \boldsymbol{G}(t)\boldsymbol{1} = \boldsymbol{0}, \forall t \in \mathbb{R} \\ & \boldsymbol{G}(t) \succeq 0, \forall t \in \mathbb{R} \\ & \max_{t \in \mathbb{R}}\ \operatorname{rank} \boldsymbol{G}(t) = d, \end{aligned} \tag{7}$$

where $\alpha_i \propto \|\widetilde{\boldsymbol{D}}_i\|_F^{-2}$ are positive weights that control the relative importance of the mismatch at different times. Since by (5) $\boldsymbol{G}(t)$ is linear in $\{\boldsymbol{G}(t)\}_{k=0}^K$, the objective in (7) is convex. Further, all constraints except the rank bound are convex.

The constraints ensure that the solution is a time-varying Gramian $\boldsymbol{G}(t)$ with correct rank. The translation ambiguity is resolved by requiring that $\boldsymbol{G}(t)\boldsymbol{1} = \boldsymbol{0}$, or equivalently $\boldsymbol{G}_k\boldsymbol{1} = \boldsymbol{0}$ for $k \in \{0, \ldots, K\}$, which implies that the recovered trajectories are centered. In practice, we discretize the continuous-time semidefiniteness constraint, and relax the non-convex rank constraint to get a convex semidefinite relaxation.

A solution to (7) is a time-varying Gramian $\boldsymbol{G}(t)$ such that the KEDM $\boldsymbol{D}(t) = \mathcal{K}(\boldsymbol{G}(t))$ best represents the measured distance sequences. Similar to the static case, the point set trajectories can be obtained by spectral factorization of the time-varying Gramian, although the latter is more challenging in the polynomial case.

4.1. Spectral Factorization with Anchor Points

Next, we show how to extract the trajectories from the estimated $\boldsymbol{G}(t)$ with the help of anchor points. In practice, anchors might correspond to nodes that are equipped with a positioning technology such as GPS. Because the anchors now move, we have more possibilities for anchor measurements than in the static case. We only need to know the positions of anchor points at some fixed, finite set of times, but we could use different sets of points at different times. However, such general anchor measurements lead to generalizations of Procrustes analysis that have no efficient solutions. Moreover, they rely on numerically unstable polynomial spectral factorization [30].

To avoid these issues, we propose a method which uses a suboptimal number of anchor measurements, but in return only requires us to factorize constant Gram matrices $\boldsymbol{G}(\tau_\ell)$ at a set of L times $\{\tau_\ell\}_{\ell=1}^L$ (that is, applied to constant matrices that are evaluations of polynomial matrices at these particular times) as $\boldsymbol{G}(\tau_\ell) = \overline{\boldsymbol{X}}(\tau_\ell)^\top \overline{\boldsymbol{X}}(\tau_\ell)$. This is easily achievable by an eigenvalue decomposition. We know that trajectories can only be estimated up to a time-invariant rotation (and possibly reflection) $\boldsymbol{U}$ and a *time-varying* translation $\boldsymbol{x}(t)$. The fact that $\boldsymbol{U}$ is a constant matrix follows from the spectral factorization theorem [31]. Given a spectral factor $\overline{\boldsymbol{X}}(t)$ of $\boldsymbol{G}(t)$, the true trajectory $\boldsymbol{X}(t)$ can be found as $\boldsymbol{X}(t) = \boldsymbol{U}\overline{\boldsymbol{X}}(t) + \boldsymbol{x}(t)\boldsymbol{1}^\top$, where $\boldsymbol{U}$ is a $d \times d$ orthogonal matrix, $\boldsymbol{x}(t)$ is a $d \times 1$ polynomial vector.

Suppose we measure positions of at least $d+1$ anchors at times $\{\tau_1, \ldots, \tau_L\}$ where $L \ge P + 1$. This allows us to use Procrustes analysis at each time τ_ℓ individually to estimate rotation and translation, $\widehat{\boldsymbol{U}}_\ell$ and $\widehat{\boldsymbol{x}}(\tau_l)$ at that time. Note that there is no guarantee that these "marginal" estimates for the rotation correspond to the unique global $\boldsymbol{U}$ we are looking for because we do not exploit any temporal model in computing the spectral factors $\overline{\boldsymbol{X}}(\tau_\ell)$. In other words, all $\widehat{\boldsymbol{U}}_\ell$ could be distinct, and in principle they will. Nevertheless, we can use them to estimate the trajectory by solving the following problem:

$$\underset{\boldsymbol{A}_p \in \mathbb{R}^{d \times N}}{\text{minimize}} \sum_{\ell=1}^{L} \left\| \sum_{p=0}^{P} \tau_\ell^p \boldsymbol{A}_p - \left(\widehat{\boldsymbol{U}}_\ell \overline{\boldsymbol{X}}(\tau_\ell) + \widehat{\boldsymbol{x}}(\tau_\ell)\boldsymbol{1}^\top \right) \right\|_F^2. \tag{8}$$

[1] In practice, we use a *pruning* method to estimate the polynomial degree P. Initialize a large P, and keep decreasing it to meet a satisfactory trajectory estimate.

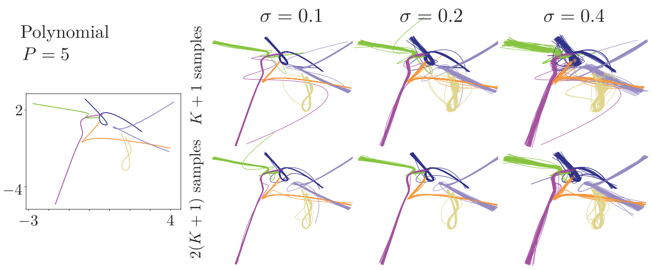

Fig. 3: Estimated trajectories, $\widehat{\boldsymbol{X}}(t)$, for $N = 6$ points in $\mathbb{R}^2$ at different levels of measurement noise and number of temporal measurements. The relative trajectory mismatches are $0.038, 0.079, 0.15$ and $0.028, 0.036, 0.084$ for $K+1$ and $2(K+1)$ measurements.

The logic behind (8) is that even though the matrices $\widehat{\boldsymbol{U}}_\ell$ are "wrong" in the sense that they do not correspond to the unique global $\boldsymbol{U}$, the aligned points $\widehat{\boldsymbol{U}}_\ell \overline{\boldsymbol{X}}(\tau_l) + \widehat{\boldsymbol{x}}(\tau_\ell)$ are correct thanks to the anchors. With sufficiently many marginal estimates, there is a unique set of polynomial trajectories passing through them. The entire trajectory localization procedure is summarized in Algorithm 1 and illustrated in Figure 1.

Algorithm 1 Solving kinetic distance geometry problem by KEDMs

(i) $(\widehat{\boldsymbol{G}}_k) \leftarrow \underset{\substack{\boldsymbol{G}_k : \boldsymbol{G}_k \succeq 0 \\ \boldsymbol{G}_k \boldsymbol{1} = \boldsymbol{0}}}{\arg\min} \sum_{i=1}^{T} \alpha_i \| \widetilde{\boldsymbol{D}}_i - \boldsymbol{W}_i \circ \mathcal{K}(\sum_{k=0}^{K} w_k(t_i) \boldsymbol{G}_k) \|_F^2$;

(ii) Given anchor positions at times $\{\tau_\ell\}_{\ell=1}^L$, solve for $\{\widehat{\boldsymbol{U}}_\ell\}_{\ell=1}^L$ and $\{\widehat{\boldsymbol{x}}(\tau_\ell)\}_{\ell=1}^L$ using Section 2.2 (Procrustes analysis);

(iii) Solve (8) for $\{\boldsymbol{A}_p\}_{p=0}^P$.

Finally, computational complexity of Algorithm 1 increases with number of moving points, N, polynomial degree, P, and number of temporal samples, T. Therefore, we have to bound these parameters in practical applications.

5. SIMULATION RESULTS

In this section we empirically evaluate the performance of the proposed algorithm under different experimental conditions. We study the effect of missing measurements and noise on the quality of the estimated trajectories. In all experiments, the distance sampling times are uniformly distributed in the interval of interest.

5.1. Noisy Measurements

We quantify the influence of noise by the relative trajectory mismatch $e_X = \int_{\mathcal{T}} \|\boldsymbol{X}(t) - \widehat{\boldsymbol{X}}(t)\|_F / \|\boldsymbol{X}(t)\|_F \, \mathrm{d}t$, which we approximate by discretizing $\mathcal{T}$. We fix a trajectory, shown in Figure 3, and a set of distance sampling times $\{t_k\}_{k=0}^K$, and generate many realizations of noisy measurement sequences $\widetilde{\mathcal{D}}_{t_0}, \cdots, \widetilde{\mathcal{D}}_{t_K}$ with the same noise variance σ^2. The iid noise is added to the non-squared distances. The empirical trajectory mismatch is an average of relative trajectory mismatches over realizations, $\frac{1}{M} \sum_m e_X^{(m)}$.

In Figure 3, we show many estimated trajectories $\widehat{\boldsymbol{X}}(t)$. As expected, the mismatch increases with measurement noise σ^2 and decreases with the number of measurements. In all cases, the estimated trajectories concentrate around the true ones.

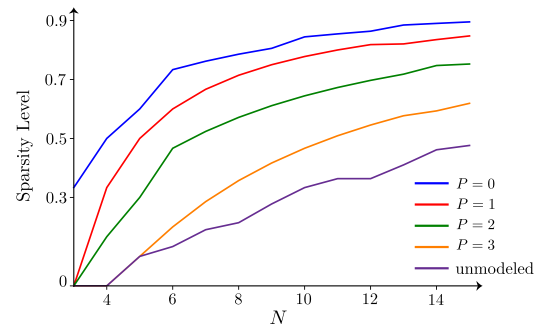

Fig. 4: The estimated sparsity level $\widehat{S}$ for polynomial degrees P and numbers of points N. The success threshold δ is set to 0.99 and the target fraction of successful reconstructions q to 0.9.

5.2. Missing Distance Measurements

Given a sequence of measurement masks $\boldsymbol{W}_1, \cdots, \boldsymbol{W}_T$, we define the sparsity level $0 \leq S \leq 1$ as the ratio of the average number of missing measurements to total number of pairwise distances:

$$S = \left[T\binom{N}{2}\right]^{-1} \sum_{i=1}^{T} \text{\# of missing measurements at time } t_i.$$

We fix the dimension $d = 2$ and the number of sampling instants $T = 7$, and vary the number of points N and the polynomial degree P. We look for the largest number of missing distances m such that the probability of successful estimation, $p(\delta, m)$, is greater than some fixed value q. We empirically estimate the success probability as $\widehat{p}(\delta, m) = \frac{M_s}{M}$ where M_s is the number of successful experiments and $M = 100$ is the number of trials for each choice of P and N. We declare an experiment successful if the relative KEDM error is below some predefined threshold δ . In practice, we run the experiment for different m and estimate:

$$\widehat{S}(\delta, q) = \frac{\widehat{m}^*(\delta, q)}{\binom{N}{2}} \text{ where } \widehat{m}^*(\delta, q) \overset{\text{def}}{=} \max\{m \,:\, \widehat{p}_M(\delta, m) \geq q\}.$$

In Figure 4, we can see that the sparsity level increases with the number of points N, and decreases with the polynomial degree P. Compared to the number of missing measurements tolerated in the static DGP, we see that KEDMs and the proposed semidefinite relaxation indeed allow us to measure few distances at any given time, and compensate for this by sampling at multiple times.

6. CONCLUSION

We presented kinetic Euclidean distance matrices—a generalization of EDMs to the case of moving points, and derived algorithms based on semidefinite programming to solve the associated trajectory localization problem. A key ingredient in our method is a representation of time-varying Gram matrices as time-varying linear combinations of constant Gram matrices. Just as in the static case, the actual localization involves an additional spectral factorization step which is not straightforward for polynomial matrices. We circumvented the related difficulties by deriving a spectral factorization method that directly uses anchor measurements. The demonstrated possibility to reduce the spatial distance sampling rate with respect to standard EDMs will be useful in situations where many distances are indeed unavailable or distance measurements are costly. Future work involves more general trajectory models and localization from relative velocities in addition to distances.

7. REFERENCES

[1] L. Liberti, C. Lavor, N. Maculan, and A. Mucherino, "Euclidean Distance Geometry and Applications," *SIAM Rev.*, vol. 56, no. 1, pp. 3–69, 2014.

[2] N. Krislock and H. Wolkowicz, "Explicit Sensor Network Localization using Semidefinite Representations and Facial Reductions," *SIAM J Optim.*, vol. 20, no. 5, pp. 2679–2708, Jan. 2010.

[3] I. Dokmanić, J. Ranieri, and M. Vetterli, "Relax and unfold: Microphone localization with Euclidean distance matrices," in *Proc. EUSIPCO*. 2015, pp. 265–269, IEEE.

[4] I. Dokmanić, R. Parhizkar, A. Walther, Y. M. Lu, and M. Vetterli, "Acoustic Echoes Reveal Room Shape," *Proc. Natl. Acad. Sci.*, vol. 110, no. 30, pp. 12186–12191, June 2013.

[5] R. Parhizkar, I. Dokmanić, and M. Vetterli, "Single-Channel Indoor Microphone Localization," in *ICASSP*. 2014, pp. 1434–1438, IEEE.

[6] L. Liberti and C. Lavor, "Open research areas in distance geometry," *arXiv*, Oct. 2016.

[7] B. Hendrickson, "The Molecule Problem: Exploiting Structure in Global Optimization," *SIAM J Optim*, vol. 5, no. 4, pp. 835–857, 1995.

[8] B. A. Hendrickson, "The Molecule Problem: Determining Conformation from Pairwise Distances," *Technical Report*, Sept. 1990.

[9] L. Liberti, C. Lavor, A. Mucherino, and N. Maculan, "Molecular distance geometry methods: from continuous to discrete," *Int. Trans. Oper. Res.*, vol. 18, no. 1, pp. 33–51, Jan. 2011.

[10] K. Menger, "Untersuchungen über allgemeine Metrik," *Math. Ann.*, vol. 100, no. 1, pp. 75–163, Dec. 1928.

[11] I. J. Schoenberg, "Remarks to Maurice Frechet's Article "Sur La Definition Axiomatique D'Une Classe D'Espace Distances Vectoriellement Applicable Sur L'Espace De Hilbert," *The Annals of Mathematics*, vol. 36, no. 3, pp. 724, July 1935.

[12] L. M. Blumenthal, *Theory and Applications of Distance Geometry*, Clarendon Press, 1953.

[13] M. Browne, "The Young-Householder algorithm and the least squares multidimensional scaling of squared distances," *J. Classification*, vol. 4, no. 2, pp. 175–190, 1987.

[14] J. C. Gower, "Euclidean Distance Geometry," *Math. Sci.*, vol. 7, no. 1, pp. 1–14, 1982.

[15] J. C. Gower, "Properties of Euclidean and non-Euclidean distance matrices," *Linear Algebra Appl.*, vol. 67, pp. 81–97, 1985.

[16] J. Dattorro, *Convex Optimization & Euclidean Distance Geometry*, Meboo, 2011.

[17] I. Dokmanić, R. Parhizkar, J. Ranieri, and M. Vetterli, "Euclidean Distance Matrices: Essential theory, algorithms, and applications," *IEEE Signal Process. Mag.*, vol. 32, no. 6, pp. 12–30, 2015.

[18] A. Cornejo and R. Nagpal, "Distributed range-based relative localization of robot swarms," in *Algorithmic Foundations of Robotics XI*, pp. 91–107. Springer, 2015.

[19] J. Matthaei, T. Krüger, S. Nowak, and U. Bestmann, "Swarm exploration of unknown areas on mars using slam," in *International Micro Air Vehicle Conference and Flight Competition (IMAV)*, 2013.

[20] J. S. Jaffe, P. J. Franks, P. L. Roberts, D. Mirza, C. Schurgers, R. Kastner, and A. Boch, "A swarm of autonomous miniature underwater robot drifters for exploring submesoscale ocean dynamics," *Nature communications*, vol. 8, pp. 14189, 2017.

[21] K. Papakonstantinou and D. Slock, "Performance bounds and identifiability conditions for location estimation in nlos dynamic environments," in *2011 IEEE Statistical Signal Processing Workshop (SSP)*. IEEE, 2011, pp. 189–192.

[22] J. Morales, P. Roysdon, Z. M. Kassas, and 2016, "Signals of opportunity aided inertial navigation," in *ION GNSS Conference*, Portland, OR, 2016.

[23] H. Durrant-Whyte and T. Bailey, "Simultaneous Localization and Mapping: Part I," *IEEE Robot Autom Mag*, vol. 13, no. 2, pp. 99–110, 2006.

[24] M. Kreković, I. Dokmanić, and M. Vetterli, "Echoslam: Simultaneous localization and mapping with acoustic echoes," in *ICASSP*, March 2016, pp. 11–15.

[25] N. Krislock and H. Wolkowicz, "Euclidean Distance Matrices and Applications," in *Handbook on Semidefinite, Conic and Polynomial Optimization*, pp. 879–914. Springer US, Boston, MA, Jan. 2012.

[26] A. M.-C. So and Y. Ye, "Theory of Semidefinite Programming for Sensor Network Localization," *Math. Program.*, vol. 109, no. 2-3, pp. 367–384, Mar. 2007.

[27] P. H. Schönemann, *A Solution of the Orthogonal Procrustes Problem With Applications to Orthogonal and Oblique Rotation*, Ph.D. thesis, University of Illinois at Urbana-Champaign, 1964.

[28] C.-C. Wang, C. Thorpe, and S. Thrun, "Online simultaneous localization and mapping with detection and tracking of moving objects: theory and results from a ground vehicle in crowded urban areas," in *IEEE Int Conf Robot Autom*. 2003, pp. 842–849, IEEE.

[29] C.-C. Wang, C. Thorpe, and A. Suppe, "Ladar-based detection and tracking of moving objects from a ground vehicle at high speeds," in *Intelligent Vehicles Symposium, 2003. Proceedings. IEEE*. IEEE, 2003, pp. 416–421.

[30] L. Ephremidze, F. Saied, and I. M. Spitkovsky, "On the algorithmization of Janashia-Lagvilava matrix spectral factorization method," *IEEE Trans. Inf. Theory*, vol. 64, no. 2, pp. 728–737, 2018.

[31] L. Ephremidze, "An elementary proof of the polynomial matrix spectral factorization theorem," *Proceedings of the Royal Society of Edinburgh Section A: Mathematics*, vol. 144, no. 4, pp. 747–751, 2014.